# Formation Pathways of Sub-Stellar Objects

Austin Rothermich

May 2024

## Contents



# 1 Introduction

## 1.1 Star Formation

The formation mechanism for stars such, as our Sun, is a fairly well understood process (Shu *et al.*, 1987). Large regions of cold, dense molecular gas and dust which are subject to gravitational perturbations (for example from a nearby star or supernova) can undergo widespread gravitational collapse. As the molecular cloud collapses into denser and denser regions, turbulence causes these dense regions to fragment into multiple pieces, which collapse into proto-stellar cores. These cores, some of which further collapses into stars, are formed with a wide range of masses. The distribution of resultant star masses from this process is known as the initial mass function (IMF), an example of which is shown in Figure 1. While the exact shape of the IMF in different star forming regions is difficult to estimate (due in part to the difficulty of observing the faint, low mass objects and the highest mass objects which have already fully evolved), the general consensus is that the star formation process makes fewer high mass objects (several tens of times the mass of the Sun) and more low mass objects (a few tenths the mass of the Sun).

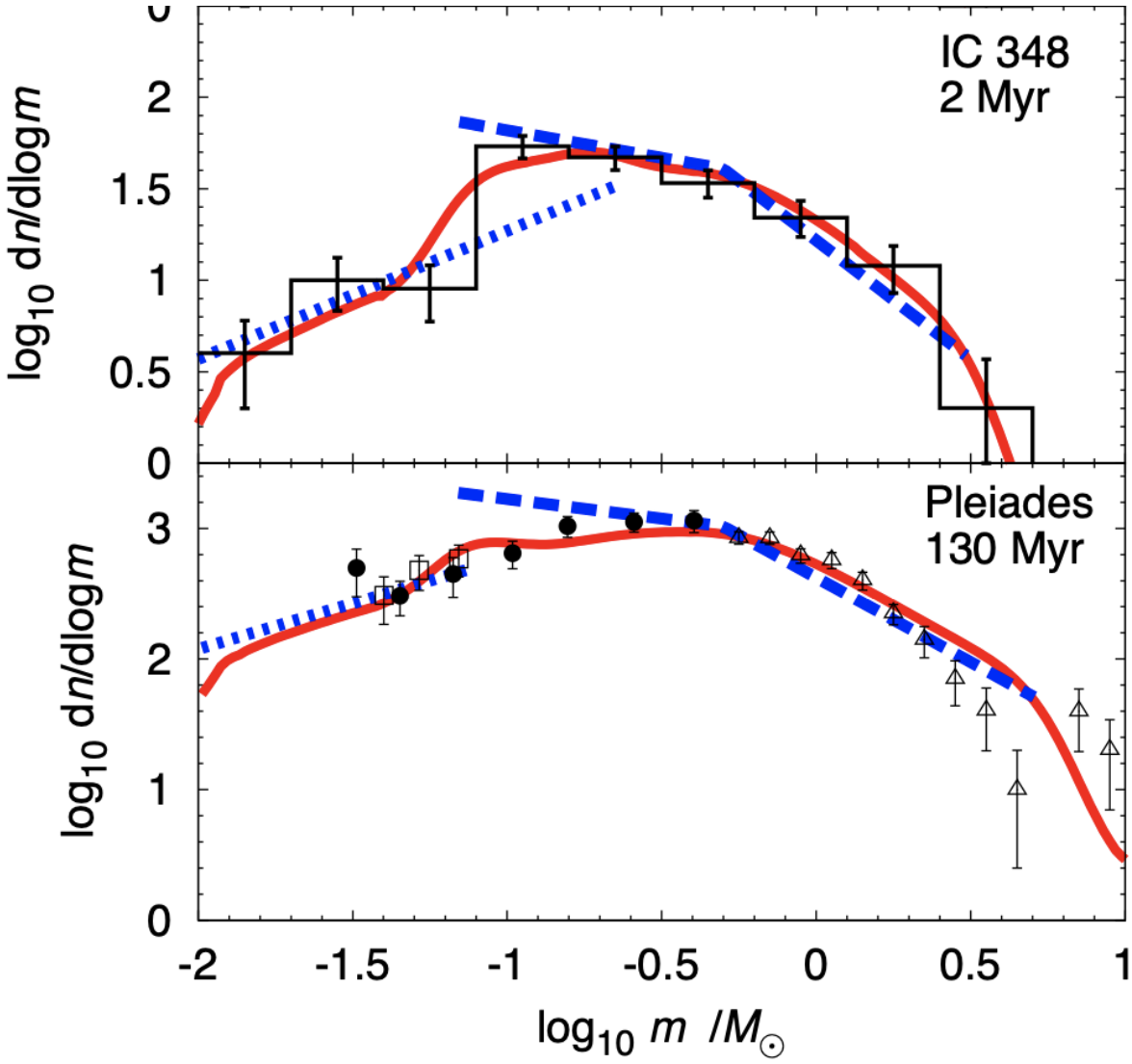


Figure 1: Example IMFs for two different star forming regions from Kroupa *et al.* (2013). Observed data points are shown in black. Model fits to different regions of the IMF are given as colored/dashed lines.

### 1.2 Sub-Stellar Objects

In the 1960's, a series of theoretical papers which were investigating the properties of the lowest mass stars made a discovery: below a certain mass, known as the hydrogen burning mass limit (HBML), a collapsing star would not have enough mass to overcome the onset of electron degeneracy pressure, resulting in an object which never attains hydrogen fusion within its core (Kumar, 1963; Hayashi & Nakano, 1963). Observed for the first time nearly 30 years later (Rebolo *et al.*, 1995; Nakajima *et al.*, 1995; Oppenheimer *et al.*, 1995), brown dwarfs now represent the lowest mass by-product of star formation. However, the discoveries of many brown dwarfs with "planetary-like masses" (as low as only a few times the mass of Jupiter) has called into question just how these objects form. While many theories exist to explain the formation of sub-stellar objects like brown dwarfs, they fall into two main scenarios: direct collapse, or gravitational instability.

In the direct collapse scenario, brown dwarfs would form through the direct collapse of the moecular cloud, through the same process as typical stars (Luhman, 2012). The proto-stellar core (or more accurately, proto-brown dwarf core) would undergo some physical process which strips it of the material necessary to

overcome the HBML. These physical processes may include situations such as the core being ejected from its natal environment, forming near a higher mass core which then steals mass from its outer regions, or even material being blown away by the winds of a nearby high mass star or supernova. Evidence points towards this being the main formation pathway of brown dwarfs, as observations of nearby star forming regions have identified proto-stellar cores and objects well below the HBML, even into the planetary mass regime (Luhman, 2012).

The gravitational instability pathway, while potentially not the main channel of brown dwarf formation, may still play a roll (if not actually becoming the dominant process) for brown dwarfs of planetary mass, as well as many directly imaged exoplanets (Luhman, 2012). In this scenario the proto-planetary disk around a newly formed star would, if certain conditions arose, become gravitationally unstable. If this instability grew, the disk could then fragment and collapse into the brown dwarf. Some of these brown dwarfs would remain as companions to the host star, with others being ejected through gravitational interactions with nearby stars.

In this paper, I will investigate some of the conditions necessary for gravitational instability to take place within a proto-planetary disk. In Section 2 I discuss the model used, as well as the assumptions needed. Section 3 presents the results from the model. Section 4 discusses some of these results in context of the results of previous studies and provides avenues for future research.

# 2 Modeling

## 2.1 Basic Assumptions

In order to investigate some of the conditions required for gravitational instability, I first started with a simple model for a proto-planetary disk. In this model, the magnetic field is ignored, as are any interactions with the host star. The sound speed ($c_s$) and surface density ($\Sigma$) as assumed constant throughout the disk.

## 2.2 Equations Used

The main parameter calculated in this paper is the Toomre "Q" stability parameter from Toomre (1964). Q is calculated from the equation:

$$Q = \frac{c_s \kappa}{\pi G \Sigma} \tag{1}$$

where $c_s$ is the sound speed of the disk, $\kappa$ is the epicyclic frequency, G is the gravitational constant, and $\Sigma$ is the surface density of the disk. If $Q \gtrsim 1$ the disk is considered gravitationally stable, whereas values of $Q \lesssim 1$ indicate the disk is unstable. However, in order to connect Q to quantities more related to observation, I followed the approach of Kratter & Lodato (2016) which approximates equation (1) as:

$$Q \approx f \frac{M_*}{M_d} \frac{H}{r} \tag{2}$$

where $M_*$ is the mass of the host star, $M_d$ is the mass of the disk, r is the radius from the star, and f is a pre-factor which depends on $\Sigma$, and is typically of order unity. As $\Sigma$ is constant in this model, we take f=1 and ignore it for the rest of the calculation. H is the "scale hight" of the disk, given by the equation:

$$H = \frac{c_s}{\Omega_K} \tag{3}$$

$$\Omega_K = \sqrt{\frac{G M_*}{r^3}} \tag{4}$$

## 2.3 Methodology

Using Q in the form of (2), three tests were performed to test the stability of the disk. Below I describe the tests performed, as well as justification for why this test is performed.

#### 2.3.1 Test 1: $M_*/M_d$

First, Q was calulated for a 1 solar mass star at a fixed radius of 100 au over a range of $M_*/M_d$ for 3 separate vales of H (through varying the value of $c_s$). This test is designed to isolate how the mass of the disk vs the mass of the star effects the stability of the disk in order to get a good idea for the general critical $M_*/M_d$ (the minimum ratio of star to disk mass which is required for gravitation instability). By varying $c_s$, which is dependent on the temperature and density of the material, this test also looks at how the critical $M_*/M_d$ changes with different disk conditions.

#### 2.3.2 Test 2: Q over all r

This test is designed as an expansion of test 1. Here, Q was calculated for a 1 solar mass star over the entire disk (out to 1,000 au) for three different values of $M_*/M_d$. This allows for an investigation into how much of the disk is unstable for different disks. In doing so this provides a basic look into how much mass the resultant sub-stellar object may have, as it will be related to how much of the disk is available to fragment. The actual mass of the fragment is not calculated in this paper, as it is beyond the scope if this work.

#### 2.3.3 Test 3: Varying Star Mass

This last test is designed to investigate whether gravitational instability of protoplanetary disks is related to the mass of the host star. Like test 2, Q was calculated for the whole disk out to 1,000 au, but this time $M_*/M_d$ was fixed at 20 for three different star masses.

# 3 Results

In this section, I present the results from the tests described in Section 2.

## 3.1 Test 1

The results from test 1 are shown in Figure 2. The Q values are represented as colored lines, and the critical value of Q=1 is shown as a gray dashed line. Starting with the disk with $c_s$=10 Km/s (representing a warm, less dense disk) we can see that over all $M_d/M_*$ Q is always greater than 1, indicating that it is gravitationally stable. As the value of $c_s$ is lowered, Figure 2 seems to indicate that lower and lower values of $M_d/M_*$ are required to become gravitational unstable. This test shows that gravitation instability prefers cool, dense proto-planetary disks.

## 3.2 Test 2

The results of the second test performed are presented in Figure 3. This test was designed to investigate the effect $M_d/M_*$ has on Q over the whole disk. Figure 3 shows that when $M_d/M_* = 0.05$, the disk is below Q=1 (unstable) out to $\sim$100 au, with Q increasing with radius beyond $\sim$100 au. As $M_d/M_*$ is lowered, less of the disk is unstable. At $M_d/M_* = 0.001$, the entire disk is stable.

## 3.3 Test 3

The results from the final test are shown in Figure 4. The goal os this test was to see if different host star masses, keeping all other parameters equal, would effect the stability of their disks. Figure 4 shows a very clear trend suggesting that host star mass does indeed play a strong roll. With $M_d/M_* = 0.05$, the 0.1 solar mass star's disk is unstable out to $\sim$5 au. The 10 solar mass star's disk however is unstable out to almost $\sim$600 au.

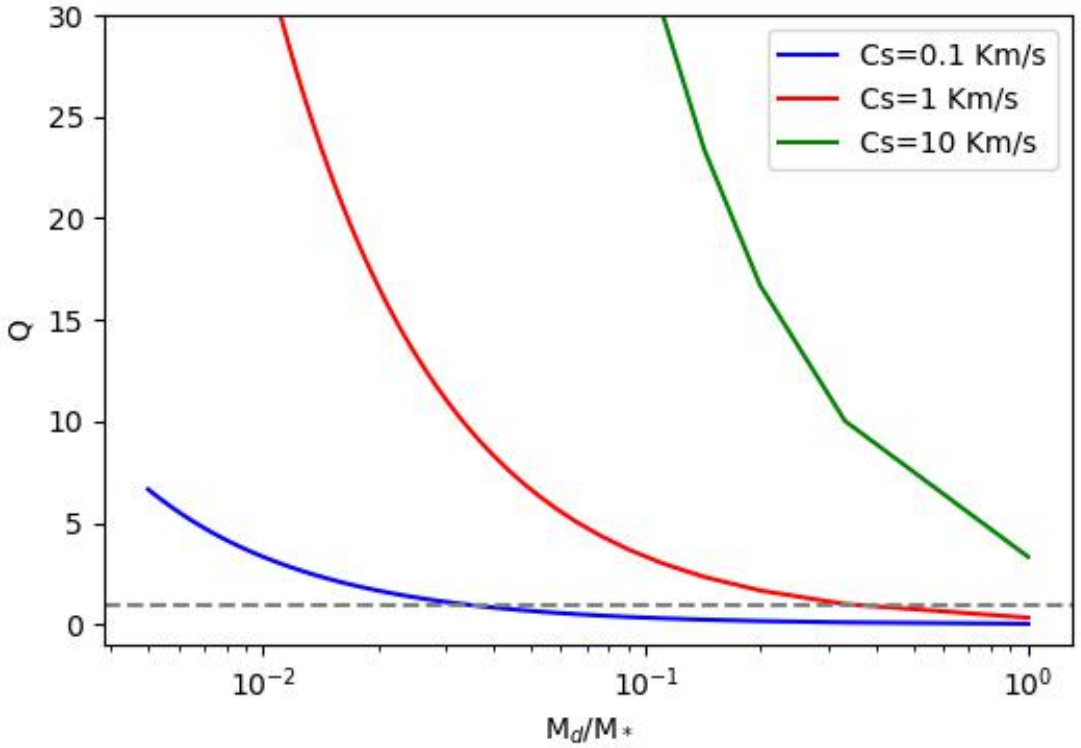


Figure 2: Q parameter vs. $M_d/M_*$ for three different values of $c_s$ shown as colored lines. The gray dashed line represents Q=1. Q was calculated at 100 au for a 1 solar mass star.

# 4 Discussion

## 4.1 Comparison to Literature

The tests performed in this paper agree that the cooler and denser the proto-planetary disk, the more likely it is to be gravitationally unstable. However, while not discussed in Section 2, gravitational instability is only one of two conditions that must be met for disk fragmentation to take place. The other condition which need to be met is $t_{cool} \lesssim t_{orb}$ (Stamatellos *et al.*, 2007), meaning that cooling time of the disk needs to be less than the orbital time of the unstable clump of the disk. While the test perfomed here doesn't address the cooling time, a cooler, denser disk will be able to more efficiently cool itself than a hotter, less dense disk. Therefore, the findings here agree with this general picture.

We can compare Figure 3 to a similar plot from Stamatellos *et al.* (2007), shown in Figure 5. Stamatellos *et al.* (2007) calculated Q using a 0.7 solar mass star with a 0.5 solar mass disk ($M_d/M_* \approx 0.7$), however unlike the simple tests run here, Stamatellos *et al.* (2007) used a time resolved hydrodynamical code which took into account all parameters of Q from equation (1) in Section 2. Looking at the first time step from Figure 5 (green line), we can see that it agrees fairly well with the general trend of Q vs r from Figure 3, with all of the disk unstable inside of ∼350 au. With increasing time in Figure 5, as material is condensed out/or accreted from the inner portion of the disk, the disk becomes more stable in those regions, culminating in the final time step (magenta) which shows the disk is stable at all radii.

The results from Figure 4 have implications for the resultant mass of the object formed from disk fragmentation. If we take a look at the 0.1 solar mass star, with a disk to star mass ratio of 0.05, this would translate to a disk mass of ∼5 Jupiter masses. Figure 4 shows that only the inner few au of the disc are

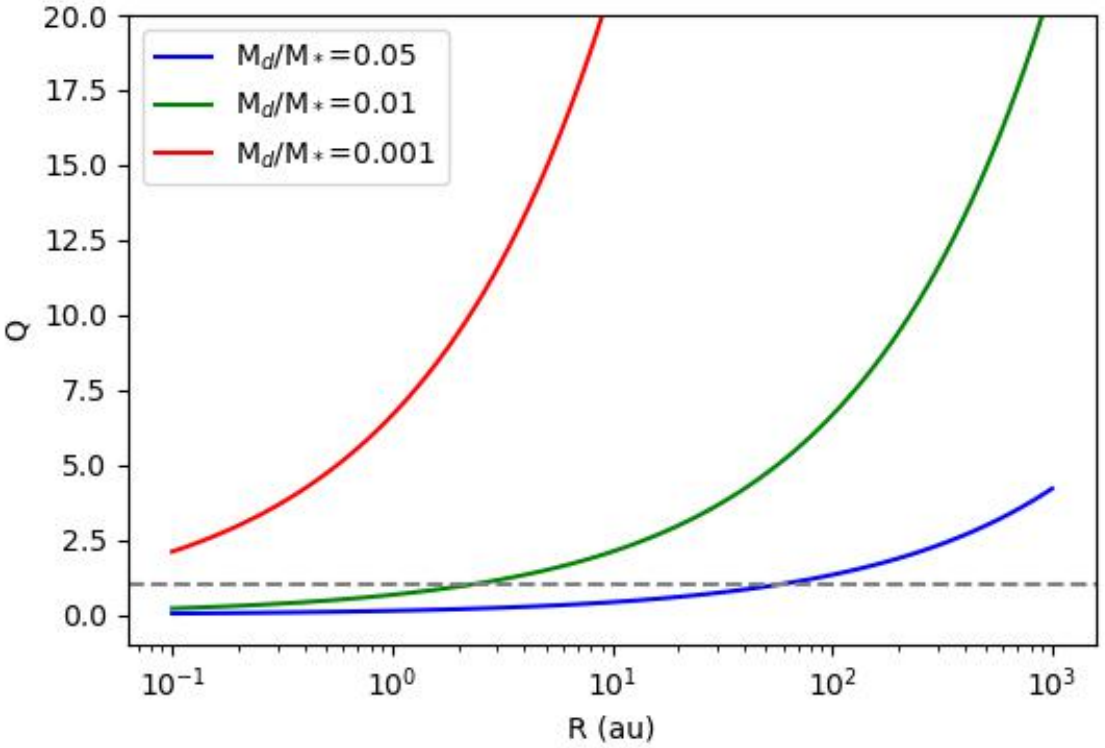


Figure 3: Q parameter vs. r for three different values of $M_d/M_*$ shown as colored lines. The gray dashed line represents Q=1. Q was calculated 1 solar mass star with $c_s$=0.2 Km/s.

unstable and susceptible to fragmentation, meaning that any object formed would have a mass less than 5 Jupiter masses. For the 10 solar mass star however, a 0.05 disk to star mass ratio translates to a disk mass of 0.5 solar masses, and Figure 4 shows that the disc remains unstable all the way out to ∼600 au. Even if only 1/5 of the disc mass fragmented off, the resultant object would have a mass above the HBML, making it a low mass star.

Stamatellos *et al.* (2007) also investigated the fragmentation masses resulting from gravitational instability, shown in Figure 6. As mentioned earlier, the disk mass used for the model in Stamatellos *et al.* (2007) was 0.5 solar masses which according to Figure 5 remains almost entirely unstable at the first time step (green line), making it analogous to the 10 solar mass star example from Figure **??**. The corresponding mass of the fragmentation in Figure 6 agrees with the argument presented in the paragraph above, with the resultant object having a mass above the HBML. In fact, even the next time step (red) results in a fragmentation above the HBML. As each time step progresses, the disk has a lower and lower mass, and therefore does not have enough mass to produce anything higher than a few Jupiter masses, similar to what was speculated about the 0.1 solar mass case from Figure 4.

## 4.2 Next Steps

There are a few next steps which could be implemented in order to further investigate fragmentation from gravitational instability. First, a full treatment of the Q parameter is needed in the model. The model used for this paper treated $c_s$ and $\Sigma$ as constants, whereas both values change with radius, so this needs to be taken into account.

As discussed earlier, the Q parameter is only one piece of the puzzle when talking about disk fragmen-

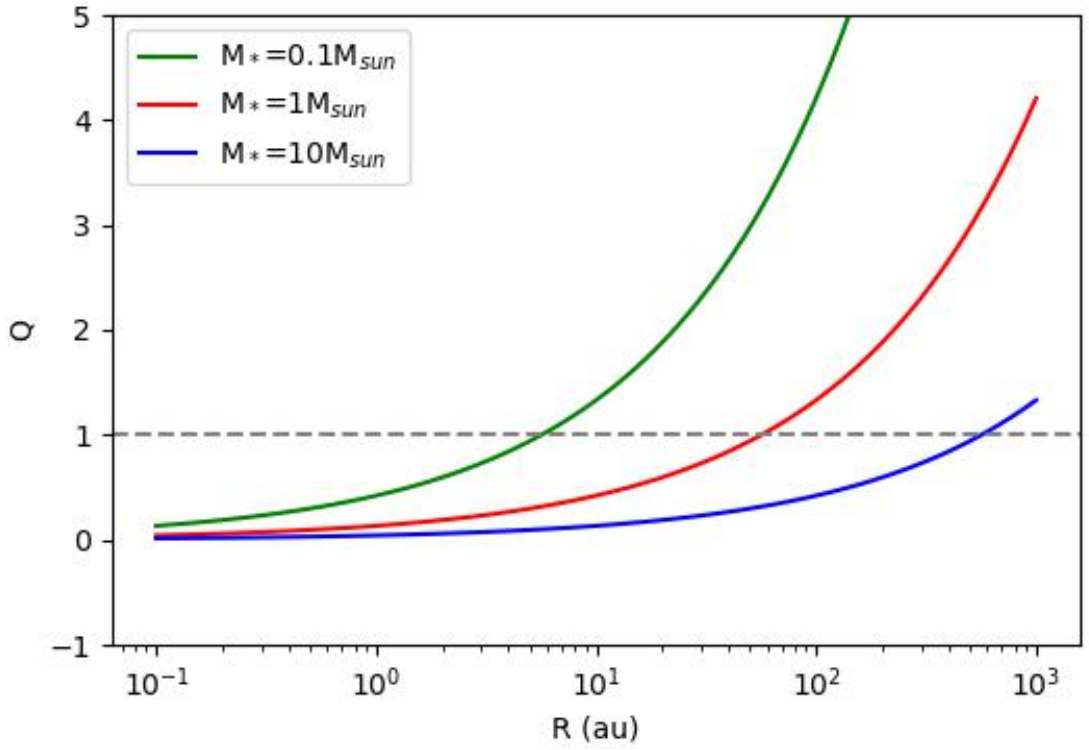


Figure 4: Q parameter vs. r for three different values of $M_*$ shown as colored lines. The gray dashed line represents Q=1. Q was calculated with $M_d/M_* = 0.05$ with $c_s$=0.2 Km/s.

tation, the other being the cooling time. future versions of this model should take this into account to be able to compute a probability of fragmentation, rather than just a stable/unstable determination.

Another helpful thing to improve the model would be to use real life disk to star mass ratios. For example, the model used in this paper used a general $M_d/M_* = 0.05$, whereas Stamatellos *et al.* (2007) used a system with $M_d/M_* = 0.05$. Without observational data, it is difficult to know which scenario better represents reality. Therefore a compilation of observed star/disk masses would be a helpful tool to begin anchoring the model with realistic parameters.

## 5 Summary

In this paper, I investigated some of the possible formation pathways of sub-stellar objects such as brown dwarfs. The mechanism explored is disk fragmentation caused by gravitational instability. I used a simplified model of a proto-planetary disk and calculated Toomre's Q stability parameter in three separate tests which vary the ratio of the disk mass to the star mass ($M_d/M_*$), the sound speed of the disk material ($c_s$), and the mass of the host star ($M_*$). These calculations show that cooler, denser disks with a higher $M_d/M_*$ or higher star masses are more susceptible to being gravitationally unstable. Comparisons with models in the literature show trends which agree with the results from this paper. Future works with this model will need to incorporate more complexity in the model, as well as anchor its parameters with those taken from observations.

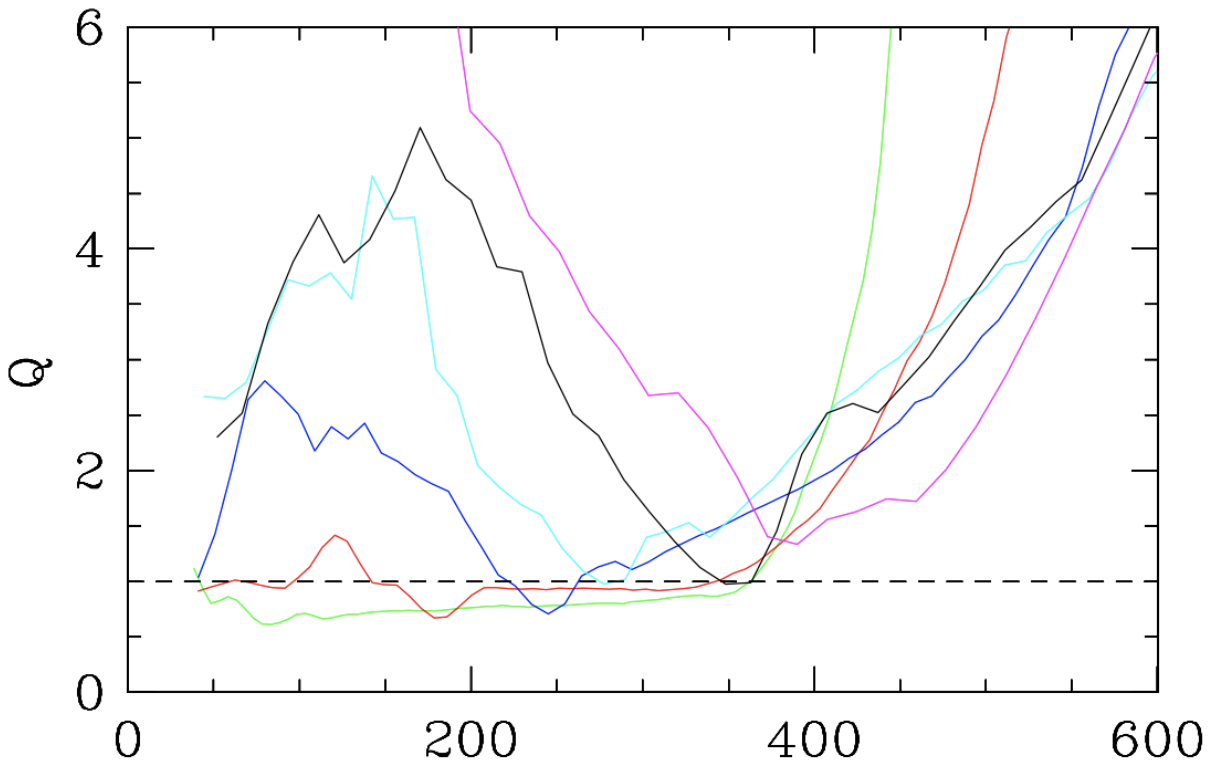


Figure 5: Figure 2a from Stamatellos *et al.* (2007) showing Q parameter vs. Each colored line represents a time snapshot of the SPH simulation (from 1000 yr to 6000 yr every 1000 yr; green, red, blue, cyan, black, magenta). The dashed line represents Q=1. Q was calculated with $M_d/M_* = 0.7$ with $M_* = 0.7$

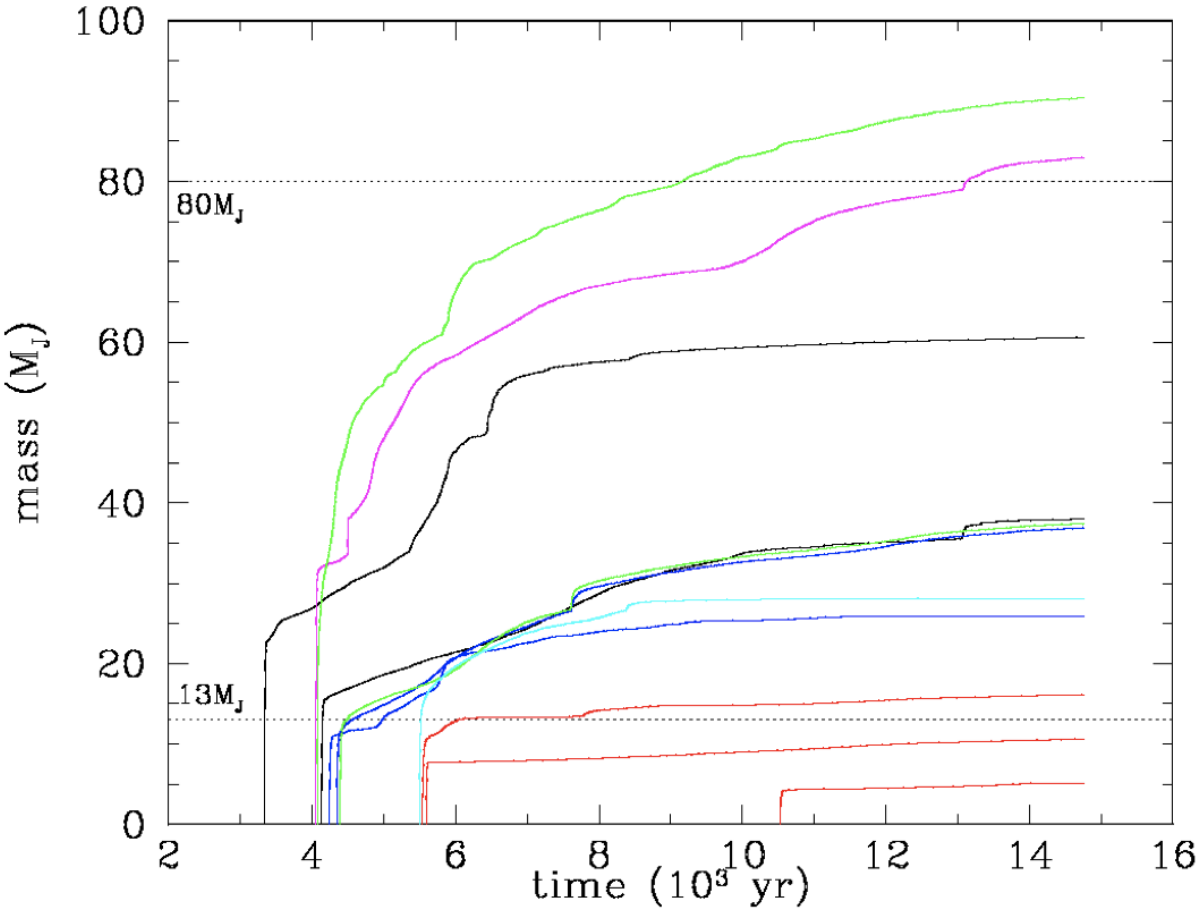


Figure 6: Figure 4 from Stamatellos *et al.* (2007) showing fragmentation masses over time. Colors of time snapshots the same as Figure 5. The dashed line represent the HBML and the dueterium burning mass limits (i.e., the mass limits of stars and planets respectively).

# References


Hayashi, C., & Nakano, T. 1963. Evolution of Stars of Small Masses in the Pre-Main-Sequence Stages. *Progress of Theoretical Physics*, **30**(4), 460–474.

Kratter, Kaitlin, & Lodato, Giuseppe. 2016. Gravitational Instabilities in Circumstellar Disks. , **54**(Sept.), 271–311.

Kroupa, Pavel, Weidner, Carsten, Pflamm-Altenburg, Jan, Thies, Ingo, Dabringhausen, Jörg, Marks, Michael, & Maschberger, Thomas. 2013. The Stellar and Sub-Stellar Initial Mass Function of Simple and Composite Populations. *Page 115 of:* Oswalt, Terry D., & Gilmore, Gerard (eds), *Planets, Stars and Stellar Systems. Volume 5: Galactic Structure and Stellar Populations*, vol. 5.

Kumar, Shiv S. 1963. The Structure of Stars of Very Low Mass. , **137**(May), 1121.

Luhman, Kevin L. 2012. The Formation and Early Evolution of Low-Mass Stars and Brown Dwarfs. , **50**(Sept.), 65–106.

Nakajima, T., Oppenheimer, B. R., Kulkarni, S. R., Golimowski, D. A., Matthews, K., & Durrance, S. T. 1995. Discovery of a cool brown dwarf. , **378**(6556), 463–465.

Oppenheimer, B. R., Kulkarni, S. R., Matthews, K., & Nakajima, T. 1995. Infrared Spectrum of the Cool Brown Dwarf Gl 229B. *Science*, **270**(5241), 1478–1479.

Rebolo, R., Zapatero Osorio, M. R., & Martín, E. L. 1995. Discovery of a brown dwarf in the Pleiades star cluster. , **377**(6545), 129–131.

Shu, Frank H., Adams, Fred C., & Lizano, Susana. 1987. Star formation in molecular clouds: observation and theory. , **25**(Jan.), 23–81.

Stamatellos, Dimitris, Hubber, David A., & Whitworth, Anthony P. 2007. Brown dwarf formation by gravitational fragmentation of massive, extended protostellar discs. , **382**(1), L30–L34.

Toomre, A. 1964. On the gravitational stability of a disk of stars. , **139**(May), 1217–1238.